Eur. Phys. J. B **23**, 201–209 (2001)

THE EUROPEAN PHYSICAL JOURNAL B

EDP Sciences

Weierstrass $\wp$-lumps

R.J. Cova[1,a] and W.J. Zakrzewski[2]

[1] Dept. de Física FEC, La Universidad del Zulia, Apartado 15332, Maracaibo 4005-A, Venezuela
[2] Dept. of Mathematics, University of Durham, Durham DH1 3LE, UK

Received 24 April 2001

Abstract. We present our results of a numerical investigation of the behaviour of a system of two solitons in the (2+1) dimensional CP^1 model on a torus. Defined by the elliptic function of Weierstrass, and working in the Skyrme version of the model, the soliton lumps exhibit splitting, scattering at right angles and motion reversal in the various configurations considered. The work is restricted to systems with no initial velocity.

PACS. 11.10.-z Field theory – 02.60.-x Numerical approximation and analysis – 03.50.-z Classical field theories

1 Introduction

Physics in (2+1) dimensions is an area of much active research, covering topics that include Heisenberg ferromagnets, the quantum Hall effect, superconductivity, nematic crystals, topological fluids, vortices and solitary waves [1]. Most of these systems are non-linear. In their mathematical description the well-known family of sigma models plays a starring role. One of the simplest models in (2+1) dimensions which is both Lorentz covariant and which possesses soliton solutions is the CP^1 or $O(3)$ sigma model. Such solutions are realisations of harmonic maps, by itself a long-established area of research in pure mathematics. However, analytical CP^1 solutions have only been found in the static (2+0) case; their dynamics is studied using numerical methods and/or other approximation techniques.

Sigma models are also useful as low dimensional analogues of important field theories in higher dimensions. In fact, the sigma CP^1 model in two dimensional space exhibits conformal invariance, spontaneous symmetry breaking, asymptotic freedom and topological solitons, properties that resemble some of those present in a number of forefront field theories in (3+1) dimensions. Amongst the latter we have the Skyrme model of nuclear physics [2]. Initially proposed as a theory of strong interactions between hadrons, it can now be regarded as a low energy limit of quantum chromodynamics [3]. The Skyrme scheme assumes that its topological solutions (skyrmions) correspond, at a classical level, to ground states of light nuclei with the topological charge (Brouwer degree) representing the baryon number. Of course, to compare with the properties of real (physical) nuclei one has to add to the classical results various quantum corrections.

Planar analogues of the Skyrme model involve the addition of some extra terms to the original CP^1 Lagrangian in order to stabilise the field solutions –the 'baby skyrmions'. Without them, the invariance of the pure, planar CP^1 theory under dilation transformations would lead to the instability of its soliton-lumps. In the traditional approach, where the solitons are harmonic maps $\Re_2 \cup \{\infty\} \approx S_2 \mapsto S_2$, one adds two terms: A Skyrme-like term which controls the shrinking of the lumps and a potential-like term which controls their expansion. Properly implemented, this procedure yields stable solitons as confirmed by numerical simulations [4].

Lately, attention has also being paid to the CP^1 model on a torus T_2 where the solitons are maps $T_2 \mapsto S_2$; this approach amounts to imposing periodic boundary conditions on the system. A characteristics of this model is that there are no solitons of topological charge one, a feature arising because $genus(T_2) = 1$.

Recent investigations have unveiled a rich diversity of phenomena in the toroidal model that goes beyond the two-lump and annular structures one might expect by analogy with the model on $\Re_2$ [5–7]. This article continues our earlier studies of CP^1 skyrmions that were found to undergo splitting when defined through the elliptic function of Weiestrass [6].

In the following section we define the toroidal CP^1 model. The numerical procedure is explained in Section 3. Section 4 reviews previous findings and presents our new results. The paper closes with Section 5, with some concluding remarks and suggestions for future research.

[a] e-mail: rcova@luz.ve

2 The CP[1] model on a torus

Our CP^1 skyrmion model is defined by the Lagrangian density

$$\mathcal{L} = \frac{|W_t|^2 - |W_x|^2 - 2|W_y|^2}{(1+|W|^2)^2} - 2\theta_1 \frac{(\bar{W}_t W_y - W_t \bar{W}_y)^2 + (\bar{W}_t W_x - W_t \bar{W}_x)^2}{(1+|W|^2)^4} + 2\theta_1 \frac{(\bar{W}_x W_y - W_x \bar{W}_y)^2}{(1+|W|^2)^4}, \quad x, y \in T_2, \tag{1}$$

which is the original CP^1 Lagrangian modified by the addition of a Skyrme, θ_1-term ($\theta_1 \in \Re$). We adopt the notation $W_t = \partial_t W, W_x = \partial_x W, W_y = \partial_y W$ for the derivatives; the bar denotes complex conjugation.

In order to obtain stable lumps on the torus it is sufficient to supplement the pure CP^1 Lagrangian with a θ_1 term as shown in equation (1). This is also the case in the (3+1) dimensional Skyrme theory. As remarked in the introduction, in order to stabilise the lumps in the traditional CP^1 model on $\Re_2$ we have to add, other than the θ_1 term, also a potential-like term.

Also it is worth mentioning that on T_2 one no longer has the problem confronted in the extended plane, whose non-compactness brings about formal difficulties in defining the metric on the moduli space of static soliton solutions [7].

For the CP^1 model to be defined on a torus we require the complex field W to obey the periodic boundary conditions

$$W[z + (m + \mathrm{i}n)L] = W(z), \qquad \forall t, \tag{2}$$

where $m, n = 0, 1, 2, ...$ and L is the size of the torus. The static solitons (instantons) are elliptic functions which may be written as

$$W = \lambda\, \wp(z - a) + b, \qquad \lambda, a, b \in \mathcal{Z}, \tag{3}$$

where $\wp$ denotes the elliptic function of Weierstrass. The partial fraction representation of $\wp$ reads

$$\wp(u) = u^{-2} - \sum_{-\infty}^{\infty} \{[u - (m + \mathrm{i}n)L]^{-2} - [(m + in)L]^{-2}\}, \tag{4}$$

the summation being over the integers m, n excluding the combination $m = n = 0$. A comprehensive treatment of elliptic functions can be found in [8,9].

The function (4) is of the second order, hence (3) represents solitons of topological charge 2. A particularity of our instantons is that they have no analytic representative of charge one (the model on $\Re_2$ has representatives in all topological classes). It is important to note that (3) is an approximate solution of the model (1), and it becomes an exact static solution in the $O(3)$ limit (θ_1=0) where it satisfies the ensuing field equation. This means that the CP^1 lumps should evolve only for $\theta_1 \neq 0$.

Our first investigations [5] of periodic solitons involved the use of the Weierstrass pseudo-elliptic function σ. Then W was taken to be given by:

$$W = \lambda \prod_{j=1}^{\kappa} \frac{\sigma(z - c_j)}{\sigma(z - d_j)}, \quad \sum_{j=1}^{\kappa} c_j = \sum_{j=1}^{\kappa} d_j, \tag{5}$$

where the accompanying selection rule between the zeroes (c_j) and poles (d_j) guarantees that W is elliptic.

Observe that when $\kappa = 1$ in (5) the constraint between the zeroes and the poles must be relaxed lest a trivial configuration W is desired. Although this procedure renders W pseudo-periodic, starting with such a field a periodic ansatz of topological charge one was constructed in [5]. This gave a field which was an approximate solution of the equations of motion for $\theta_1 \neq 0$, but became singular as $\theta_1 \to 0$.

The power series for σ on a square torus may be cast into the form

$$\sigma(u) = \sum_{j=0}^{\infty} G_j u^{4j+1}, \qquad G_j \in \Re. \tag{6}$$

With the help of equation (4) the coefficients G_j can be calculated by expanding

$$\sigma(u) = \int_0^u [\wp(v) - 1/v^2].$$

In general, the coefficients are written in terms of the so-called *invariants* $g_2(L)$ and $g_3(L)$. However, square boundary conditions effectively set $g_3 = 0$, the lemniscate case, leading to a relatively simple expression of the form (6).

Let us also add that we can re-express the $\wp$ function through σ *via* the formula

$$\wp(u) = -\frac{\mathrm{d}^2}{\mathrm{d}u^2} \ln[\sigma(u)], \tag{7}$$

and then perform the computation of σ with the same numerical subroutine which was used in reference [5].

Note that each factor $\sigma(u)/\sigma(v)$ in the field (5) can be used to represent a single soliton, providing a setting to studying more or less independent lumps in all topological classes. Solitons in the σ-picture may, for example, be boosted independently. On the other hand, through equation (3) we can only have solitons of even topological index because $\wp$ is itself an elliptic function of order two. Lumps in the $\wp$-picture are less independent than their siblings in the σ-formulation, for changing the values of the parameters in (3) always affects *both* lumps. Strictly speaking, however, truly independent solitons can only be obtained in the asymptotic regime of large lump separation, which really never happens on a compact manifold [10].

Now let us display some useful relations satisfied by the $\wp$ function, relations which follow from (4). They are:

$$\wp(-u) = \wp(u), \quad \wp(\mathrm{i}u) = -\wp(u), \quad \wp(\bar{u}) = \overline{\wp(u)}. \tag{8}$$

Moreover, there exists a useful algebraic relation between $\wp$ and $\mathrm{d}\wp/\mathrm{d}u$ on a square torus which reads

$$[\frac{\mathrm{d}\wp(u)}{\mathrm{d}u}]^2 = 4\wp(u)[\wp(u)^2 - \wp(L/2)]. \tag{9}$$

It can be deduced from the equations (8) and (9) that the function $\wp$ is purely imaginary on the diagonals bisecting the fundamental cell and real on the central cross and on the boundary of the cell:

$$\wp = \begin{cases} \text{imaginary: on central diagonals;} \\ \\ \text{real:} \qquad\quad \text{on central cross and boundary.} \end{cases} \tag{10}$$

The static energy density associated with the field (3) can be read-off from the Lagrangian density (1). Using formula (9) we may write

$$\begin{aligned} E &= e(1 + 4\theta_1 e), \\ e &= 8\lambda^2 \frac{|\wp(z-a)||\wp^2(z-a) - \wp^2(L/2)|}{[1 + |\lambda\wp(z-a) + b|^2]^2}\,. \end{aligned} \tag{11}$$

Pictures of E reveal a distribution of lumps localised in space. The parameter λ is related to the size of the lumps, b determines their mutual separation and the parameter a merely shifts the system as a whole on the torus. Throughout our simulations we have chosen the values

$$\lambda = (1, 0), \quad a = (2.025, 2.05), \quad \theta_1 = 0.001 \text{ (or zero)},$$

and studied different configurations by varying b.

3 Basic numerical set up

We have taken fields of the form (3) as the initial conditions for our time evolution, studied numerically. Since the field W may become arbitrarily large, we have preferred to run our simulations in the ϕ-formulation of the model. Its field equation follows from the Lagrangian density (1) with the help of the stereographic projection

$$\boldsymbol{\phi} = (\underbrace{\frac{W + \bar{W}}{|W|^2 + 1}}_{\phi_1}, \ \underbrace{\mathrm{i}\frac{-W + \bar{W}}{|W|^2 + 1}}_{\phi_2}, \ \underbrace{\frac{|W|^2 - 1}{|W|^2 + 1}}_{\phi_3}), \tag{12}$$

with the real scalar field $\boldsymbol{\phi}$ satisfying $\boldsymbol{\phi}\cdot\boldsymbol{\phi} = 1$. One has

$$\begin{aligned} \mathbf{0} = {} & (\partial^\mu\partial_\mu - \boldsymbol{\phi}\cdot\partial^\mu\partial_\mu\boldsymbol{\phi})\boldsymbol{\phi} + 2\theta_1[\partial^\mu\partial_\mu\boldsymbol{\phi}(\partial^\nu\boldsymbol{\phi}\cdot\partial_\nu\boldsymbol{\phi}) \\ & + \partial_\nu\boldsymbol{\phi}(\partial_\mu\partial^\nu\boldsymbol{\phi}\cdot\partial^\mu\boldsymbol{\phi}) - \partial_\nu\partial_\mu\boldsymbol{\phi}(\partial^\nu\boldsymbol{\phi}\cdot\partial^\mu\boldsymbol{\phi} \\ & - \partial^\mu\boldsymbol{\phi}(\partial_\nu\partial^\nu\boldsymbol{\phi}\cdot\partial^\mu\boldsymbol{\phi}) + (\partial^\mu\boldsymbol{\phi}\cdot\partial_\mu\boldsymbol{\phi})(\partial^\nu\boldsymbol{\phi}\cdot\partial_\nu\boldsymbol{\phi})\boldsymbol{\phi} \\ & - (\partial_\mu\boldsymbol{\phi}\cdot\partial_\nu\boldsymbol{\phi})(\partial^\mu\boldsymbol{\phi}\cdot\partial^\nu\boldsymbol{\phi})\boldsymbol{\phi}], \end{aligned} \tag{13}$$

where $\mu, \nu = 0, 1, 2$ are the Lorentz indices; as usual we have $t, x, y = x^0, x^1, x^2$.

We compute the series (6) up to G_5, the coefficients G_j being in our case negligibly small for $j > 5$:

$$\left.\begin{aligned} G_0 &= 1 \\ G_1 &= -0.7878030 \\ G_2 &= -0.221654845 \\ G_3 &= 9.36193 \times 10^{-3} \\ G_4 &= 7.20830 \times 10^{-5} \\ G_5 &= 2.37710 \times 10^{-5} \end{aligned}\right\}.$$

We have employed the fourth-order Runge-Kutta method and approximated the spatial derivatives by finite differences. The Laplacian has been evaluated using the standard nine-point formula and, to further check our results, a 13-point recipe has also been used. Respectively, the Laplacians are:

$$\nabla^2 = \frac{\begin{bmatrix} 1 & 4 & 1 \\ 4 & -20 & 4 \\ 1 & 4 & 1 \end{bmatrix}}{6 \times a^2},$$

$$\nabla^2 = \frac{\begin{bmatrix} & & -1 & & \\ & 1 & 12 & 1 & \\ -1 & 12 & -48 & 12 & -1 \\ & 1 & 12 & 1 & \\ & & -1 & & \end{bmatrix}}{10 \times a^2}.$$

The discrete model has been evolved on a $n_x \times n_y = 200 \times 200$ periodic lattice with spatial and time steps $\delta x{=}\delta y = 0.02$ and $\delta t = 0.005$, respectively. The vertices of the fundamental lattice we have used for our simulations were at

$$(0,0),\ (0,L),\ (L,L),\ (L,0), \quad L = n_x \times \delta x = 4. \tag{14}$$

Unavoidable round-off errors have gradually shifted the fields away from the constraint $\boldsymbol{\phi}\cdot\boldsymbol{\phi} = 1$. So we rescale

$$\boldsymbol{\phi} \to \boldsymbol{\phi}/\sqrt{\boldsymbol{\phi}\cdot\boldsymbol{\phi}}$$

every few iterations. Each time, just before the rescaling operation, we evaluate the quantity $\mu \equiv \boldsymbol{\phi}\cdot\boldsymbol{\phi} - 1$ at each lattice point. Treating the maximum of the absolute value of μ as a measure of the numerical errors, we find that $\max|\mu| \approx 10^{-8}$. This magnitude is useful as a guide to determine how reliable a given numerical result is. Usage of an unsound numerical procedure in the Runge-Kutta evolution shows itself as a rapid growth of $\max|\mu|$; this also occurs, for instance, in the limit $\theta_1 \to 0$ when the unstable energy lumps become infinitely spiky.

4 Results

In reference [6] we considered two cases: $b = (0, 0)$ and $b = (1, 0)$. For $\boxed{b = (0,0)}$ one has a most evenly spread

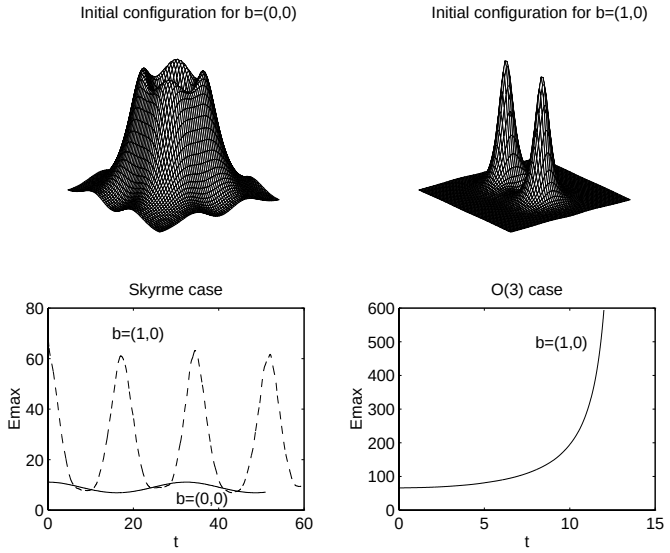

Fig. 1. Energy density configurations at $t = 0$ and the evolution of the maximum $E_{\max}$. Above we see the special case featuring four lumps $[b = (0, 0)]$ and the more common situation with a pair of lumps $[b = (1, 0)]$. The evolution of $E_{\max}$ is illustrated bellow, both for the Skyrme and pure $O(3)$ case. The instability of the latter is manifest by the lumps shrinking non-stoppingly.

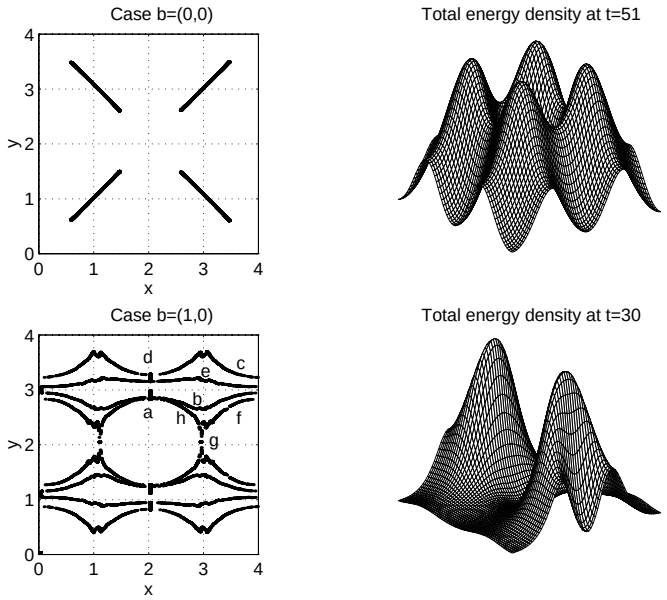

Fig. 2. Above: Skyrmion for the exceptionally symmetric case $b = (0, 0)$. The four lumps stay on the diagonals and move towards the corners and coalesce. They break-off again and proceed back to the centre of the lattice at $t = 51$. Below: The $b = (1, 0)$ skyrmions split each in two lumps that transit complicated paths; the labels $a - h$ refer to one of the 'half-lumps'. The $t = 30$ picture features the situation shortly after the 'fractional' lumps reunite at d (and at its symmetrical point) and begin to travel centrewards.

energy distribution. Notably, this homotopy-two class configuration exhibits *four lumps* (rather than two) sitting on the central diagonals of the basic grid (14). (See the top-left graph of Fig. 1.) When evolved from rest in the Skyrme scheme, this quartet has moved along the diagonals under the action of a net repulsive force. They have evolved in a manner that resembled a scattering at right angles as illustrated in upper half of Figure 2. No splitting has been observed.

The state $\boxed{b = (1, 0)}$ corresponds to a couple of lumps placed along the coordinate axes as seen in Figure 1 (top-right). This is certainly a more familiar picture for solitons belonging to a charge-two topological sector. Unfamiliar, though, is their novel dynamics: starting from rest after a while each soliton splits into two lumps. The split is in the direction perpendicular to the line joining the solitons. As time goes by, the offspring skyrmions glue back together, split again and so forth. This is depicted in the lower part of Figure 2 and is the splitting phenomenon described in the introduction. The time at which the lumps begin to split is $t \approx 7$.

The lower half of Figure 1 shows plots of $E_{\max}\, vs.\, t$ for the above cases, including the unstable $O(3)$ case. In the latter, as expected, the lumps do not move at all (let alone split) with the passing of time – as long as the initial speed is zero. This is in accordance with our expectations, for, as we recall, the field (4) is a static solution of the pure $O(3)$ model.

Note that in general $b = (\alpha, 0)$ corresponds to solitons initially located on the central cross of the grid. If $\alpha > 0$ ($\alpha < 0$) the lumps lie on the vertical (horizontal) axis. Our qualitative results are unaffected by reasonable values of α. In connection with these configurations it is interesting to consider the case where the simulations run in the Skyrme format up to $t = t_0$, after which they evolve with $\theta_1 = 0$. In other words, we perform the simulations with a Skyrme field as the initial condition for the $O(3)$ evolution. Since the splitting forces act only when $\theta_1 \neq 0$, we expect that the larger t_0 is the sooner the solitons will begin to divide up.

Let us analise the situation arising from $\boxed{b = (-1, 0)}$, which positions the lumps along the horizontal axis. Figure 3 illustrates the evolution of the system for the sample cases $t_0 = 1.3, 1.5$. We find that after splitting the extended structures reunite but eventually break up for good. In agreement with our estimates, for $t_0 = 1.3$ the system splits later than it does for $t_0 = 1.5$. Also apparent is that the lumps show a stronger tendency to glue back in for $t_0 = 1.3$. We may now compare these plots with Figure 4, which exhibits the splitting situation for $b = (-1, 0)$ in the limit $t_0 = \infty$, *i.e.,* when the routine evolves with the Skyrme term on at all times.

The previous diagrams suggest that a t_0 might exist for which the lumps would come back together without further division. After some trial and error we have found that such critical time is approximately $t_0 \approx 1.25$. The plots presented in Figure 5 show that the forces brought about by the skyrmionic initial conditions are just enough to set the solitons oscillating in a break-up-join-up fashion. The skyrmions eventually settle together and stay

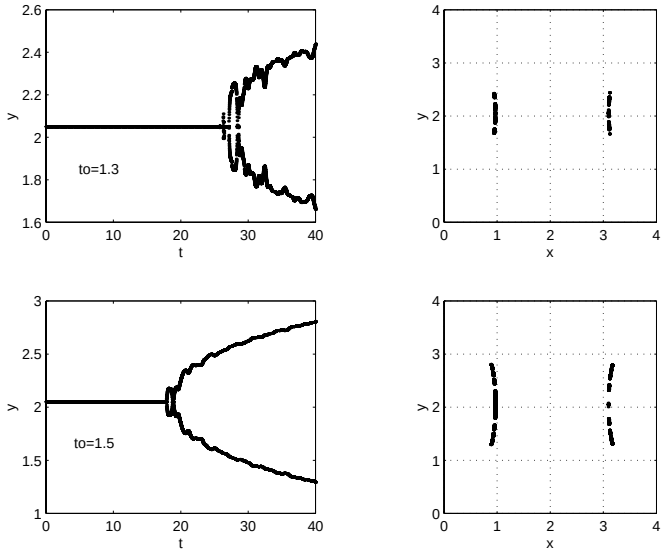

Fig. 3. The CP^1 solitons $b = (-1, 0)$ are run with $\theta_1 \neq 0$ (Skyrme format) up to $t = t_0$, at which time θ_1 is set to zero (pure format). As expected, the lumps divide up more readily for larger t_0. The change in the vertical coordinate of $E_{\max}$ as time goes by, and the trajectory plots for the two cases $t_0 = 1.3, 1.5$ are shown.

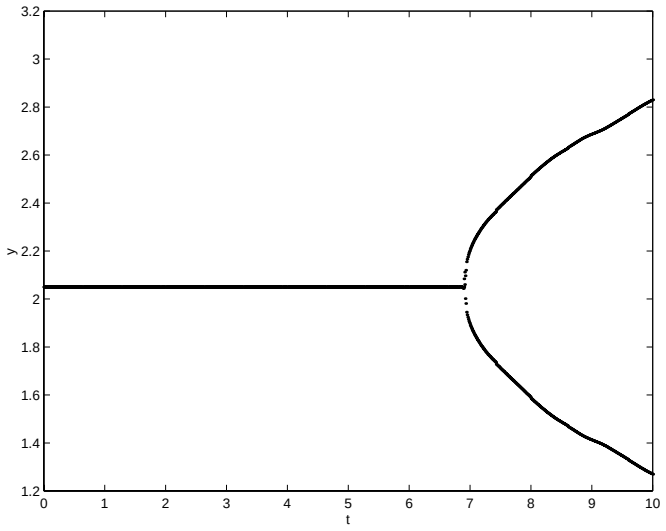

Fig. 4. Featuring the division of solitons for $b = (-1, 0)$ as in Figure 3, but with the Skyrme term on at all times.

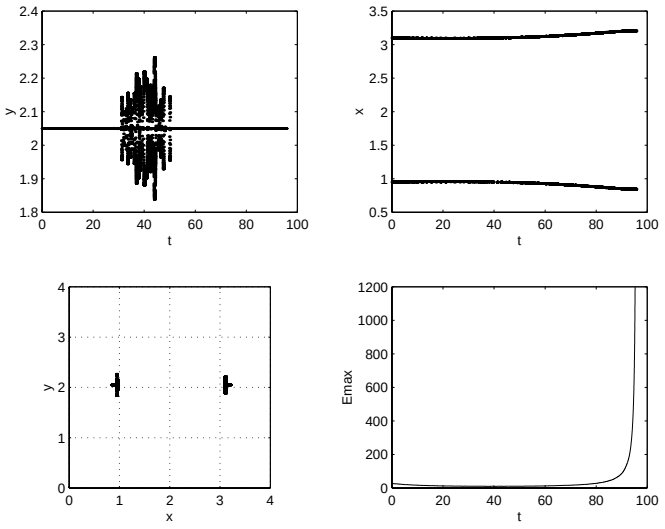

Fig. 5. For the critical time $t_0 \approx 1.25$ the energy lumps of Figure 3 can be forced back together.

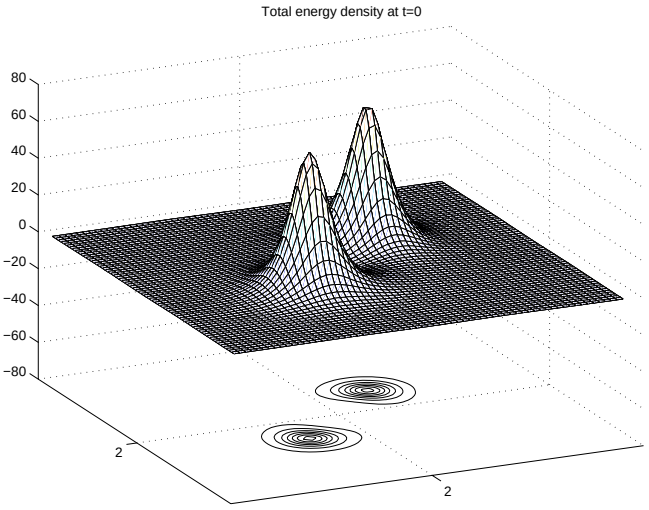

Fig. 6. Energy distribution, equation (11), for $b = (0, 1)$. The extended structures sit along the main diagonals of the lattice. Starting off from rest, these entities attract each other, collide at the centre of the grid and scatter at right angles with respect to the initial direction of motion. (See Fig. 7.)

that way for as long as the numerical procedure can be trusted: In the pure format $E_{\max}$ shrinks indefinitely as usual although it takes quite a while for the system to blow up ($t \approx 100$). This soliton is almost a static solution of the model.

Let us point out that when defined *via* equation (5) the periodic chunks of energy were found not move at all when $v_0 = 0$, neither in the pure case nor in the Skyrme case [5]. Such result is rather unexpected for skyrmions, for they are only approximate solutions of the field equation. Therefore, solitons obeying (2) look sensitive to the choice of function describing them. Not so on $\Re_2$, where the behaviour of the solitons is qualitatively the same for all the choices.

Let us now study $\boxed{b = (0, 1)}$. For this value the energy distribution (11) associated with (3) has the form of two lumps placed on a bisecting diagonal of the elementary grid (Fig. 6). Our numerical simulations show that the skyrmions attract each other and collide at the centre of the grid. They coalesce indistinguishably for a moment and then re-emerge perpendicularly to the initial line of approach, scattering off at 90°. Afterwards they continue towards the corners (which are the same point in a periodic set-up like ours) where they again scatter off at 90°.

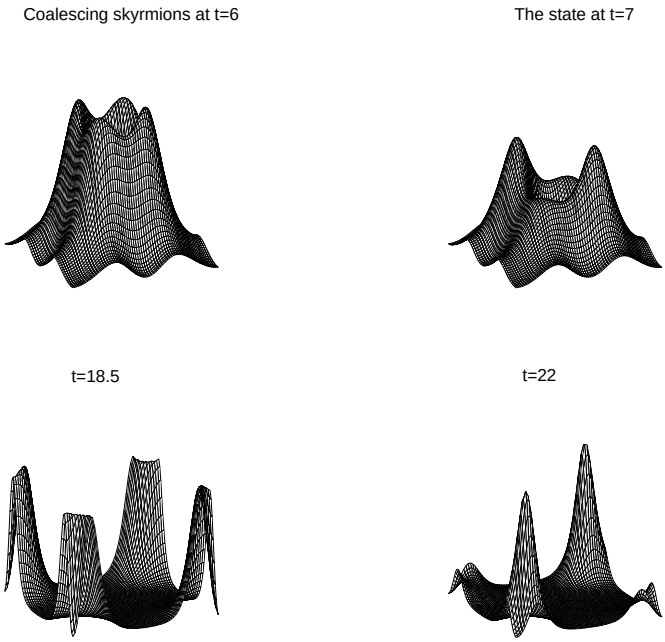

Fig. 7. The solitons of picture 6 collide at the centre ($t = 6$) and scatter off at right angles ($t = 7$). A similar event occurs at the corners ($t = 18.5$), after which the solitons proceed back to the centre. Such scatterings take place time and again, in periodic cycles. No splitting is detected.

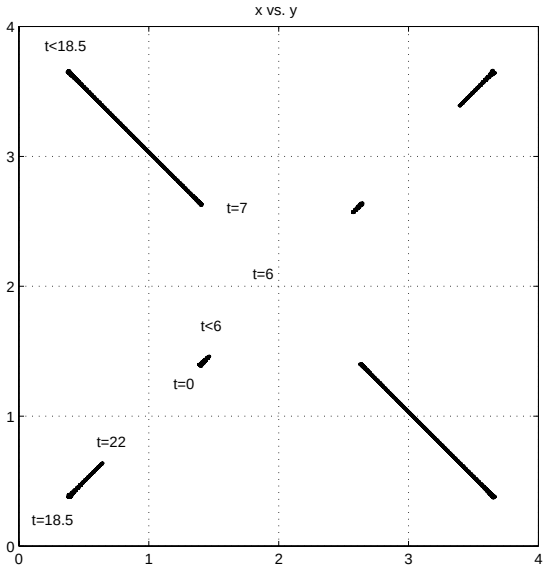

Fig. 8. Trajectory plot further illustrating the $b = (0, 1)$ lumps described in the previous picture, Figure 7. The Skyrme term introduces forces that make the lumps cruise along the diagonal and collide head-on ($t = 6$). The scattering at ninety degrees is apparent: Around $t = 18.5$ the skyrmions bump into each other at the corners $(x, y) = (0, 4)$,(4,0), re-emerging perpendicularly through $(x, y) = (0, 0)$,(4,4).

These events are depicted in Figures 7 and 8; the corresponding $E_{\max}(t)$ diagram is the Skyrme curve shown in the lower half of Figure 9. Such multi-scattering process goes on indefinitely, and no splitting is observed.

We have also evolved the $b = (0, 1)$ case with $\theta_1 = 0$. This time the energy chunks have not moved at all with the passing of time until they have become too narrow and the numerical procedure has broken down (see Fig. 9). The shrinking of solitons and the problem of singularity formation in this model was predicted in [7], using the geodesic approximation.

Next we consider $\boxed{b = (1, 1)}$. Here we have a pair of lumps initially situated at some almost random points, neither on the central cross nor on the central diagonals of the lattice. Figures 10 and 11 reveal an interesting evolution for these skyrmions. As time elapses they move along the flat torus along the x-axis, disappearing/re-appearing through the lateral edges of the basic cell (14) in a continuous, periodic motion. For instance, the skyrmion at the upper (lower) half of the grid journeys towards decreasing (increasing) x whilst keeping its y coordinate roughly constant. The lump disappears into the line $x = 0$ ($x = 4$) re-emerging from the opposite side $x = 4$ ($x = 0$). By imagining the flat torus as the product manifold of two circles, $T_2 = S_1 \times S_1$, we can visualise the motion just described as the trajectory on a circle with our x coordinate corresponding to an angle.

The two lumps continue moving along and, around $t = 69.5$, they reverse their motion: The skyrmion at the upper (lower) half of the grid starts towards increasing (decreasing) x whilst keeping its y coordinate roughly

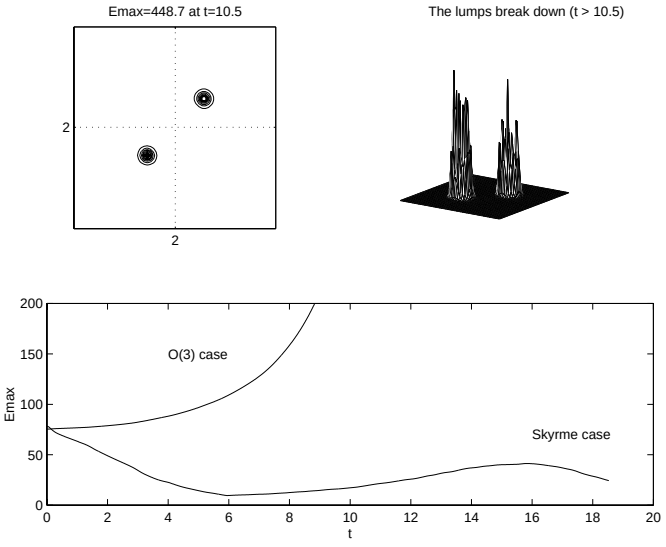

Fig. 9. Pure CP^1 case corresponding to the value $b = (0, 1)$. The lumps stay still at their initial positions (top-left) as time elapses. They break down as illustrated at the top-right diagram. Below we have the evolution of $E_{\max}$, including the Skyrme case.

constant. Now the upper (lower) lump will disappear through the line $x = 4$ ($x = 0$) and re-emerge on the opposite side $x = 0$ ($x = 4$). Figure 12 presents the variation of the coordinates in time, as well as the evolution of the peak of the energy density. No splitting was observed for fields of the type $b = (1, 1)$.

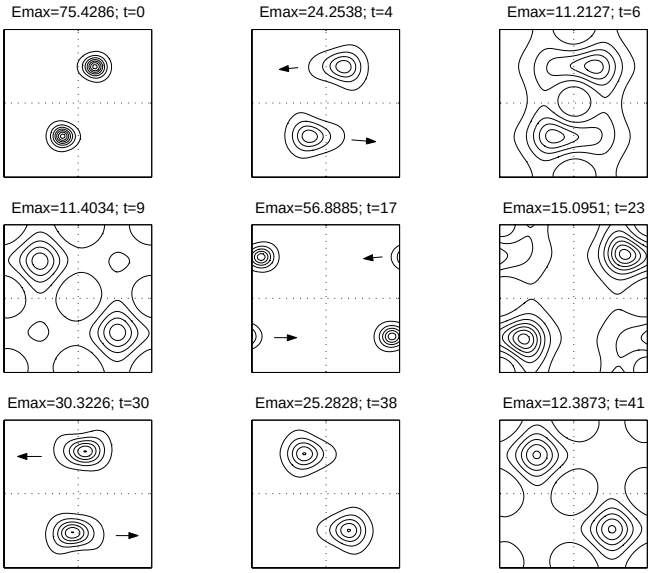

Fig. 10. Showing the dynamics arising from $b = (1, 1)$. Although no initial speed is impinged on this system, the skyrmions move resembling a collision at a certain impact parameter. One skyrmion moves towards decreasing x whereas the other skyrmion proceeds in the sense of increasing x. The disappearance/appearance of the lumps through the edges of the lattice reflects the periodicity of the network (14).

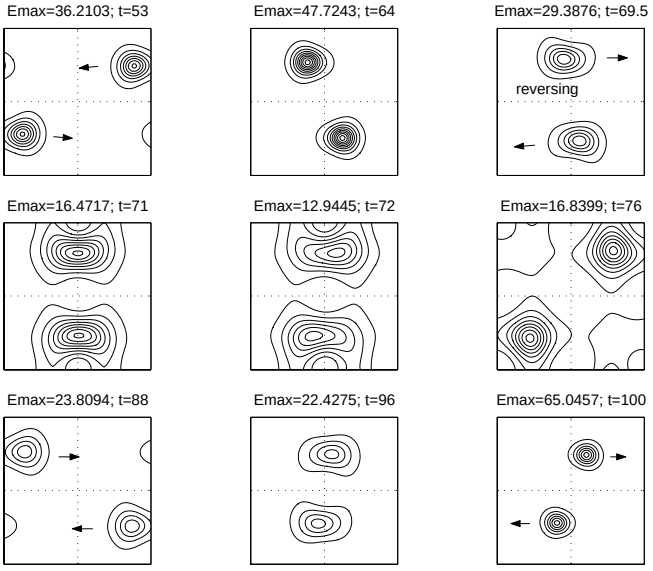

Fig. 11. Motion reversal: The skyrmionic structures of Figure 10 continue their itinerary but, at $t = 69.5$, their motion begins to reverse.

Thus, for skyrmions whose initial positions are determined by $b = (\alpha, \beta)$ our results indicate that

- *splitting only occurs* for $b = (\alpha, 0)$, $\alpha \neq 0$, that is, when the solitons originally lie on the central cross of the network (14). A repulsive, splitting force acts *within* each lump. By using a Skyrme field as an initial condition for the $O(3)$ evolution, it is possible to introduce some attractive forces so that the lumps stick back together.
- *Head-on right angle scattering only takes place* for $b = (0, \beta)$, that is, when the skyrmions initially sit on the central diagonals of the grid. There is a net attractive force between the lumps. Now,
  - if $\beta \neq 0$ then we have two lumps located on a diagonal;
  - if $\beta = 0$ then we have four lumps symmetrically situated on both main diagonals. In this case, the scattering becomes a breather-like vibration with the four lumps moving in towards the centre of the grid and moving out again. Interestingly, a look at the property (10) indicates that for b=(0,0) the soliton $W = \wp(z - a)$ is purely imaginary.
- *Neither splitting nor scattering* is observed when $b = (\alpha, \beta)$, $\alpha, \beta \neq 0$. Here we have a configuration of two energy humps propelled along the lines parallel to the edges of the cell and, later on, experiencing a 180° change in their sense of motion. This looks like scattering at a large impact parameter. We remark that all systems considered in the present paper start off from rest.

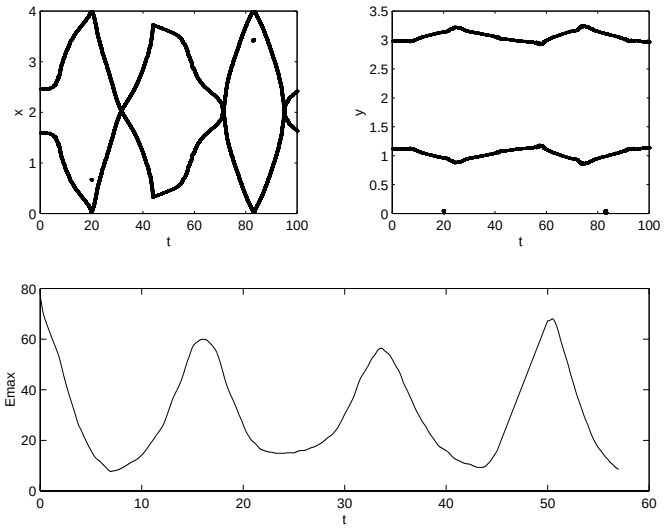

Fig. 12. Above: The evolution of the coordinates of $E_{\max}$ corresponding to the event depicted in Figures 10 and 11. Below: The evolution of $E_{\max}$ itself.

The right angle scattering is a generic feature of sigma-type models [12]. In the case of the CP^1 dynamics on T_2 the scattering at 90° was theoretically hinted at in [7] (pure case), where the initial value problem was defined in terms of the $\wp$ function (4); the solitons were evolved using the geodesic approximation. In reference [11] we evolved the $\wp$ solitons using a numerical simulation of the full CP^1 model (pure case) and confirmed the 90° scattering predictions of [7]. Earlier on [5], we had observed the said scattering on T_2 (for both the pure and Skyrme cases) with solitons expressed through the σ function (6). The present work further establishes these results, with the added interesting feature that the lumps, in the Skyrme

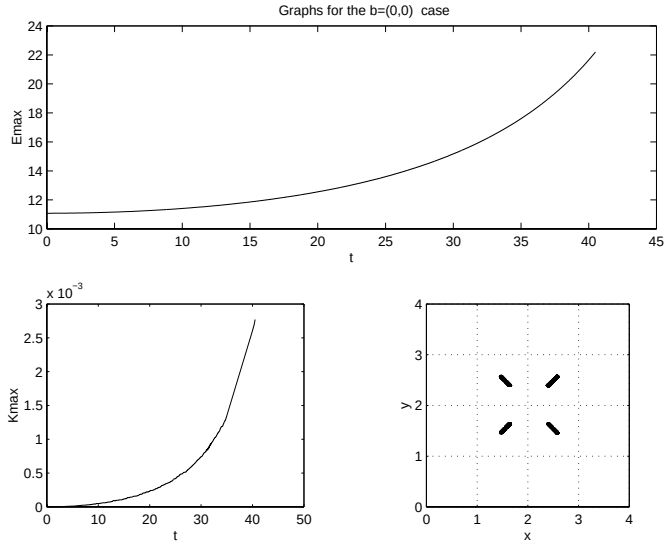

Fig. 13. Illustrating the alluring 4-lump, charge-2 state for the $\theta_1 = 0$ case. It is an almost stable configuration. The system moves out and in along the diagonals oscillating in a breather-like fashion.

case, collide and scatter off even though they have no initial speed.

Among other sigma models that exhibit 90° scattering we can mention monopoles [13] and vortices [14].

Finally, it is worth to note from the bottom-left diagram of Figure 1 that the lumps for the $b = (0, 0)$ case shrink very little, which suggests quite a stable configuration. So we have performed a number of simulations with $b = (0, 0)$ in the pure $O(3)$ format. Indeed, as Figure 13 shows, the solitons shrink at a very slow rate and can be regarded as stable for practical purposes. Contrary to the case of $\theta_1 = 0$ processes with no initial speed, a displacement in this four-lump configuration is observed, one of breather-like characteristics.

5 Concluding remarks

The CP^1 model in (2+1) dimensions has a very rich structure. On the torus we have uncovered several characteristics qualitatively different from those seen in the usual model on the compactified plane. For example in the two skyrmion sector there exits a configuration featuring four lumps rather than two. (Clearly, care should now be exercised when referring to the topological charge as the 'lump number'.) We also have the interesting fact that no one soliton solutions exist on T_2. The lumps are not stable in the pure $O(3)$ set-up, but become stable in the Skyrme model, constructed by the addition of just one extra term to the $O(3)$ Lagrangian.

Skyrmions on T_2 have many other important properties. For instance, their behaviour depends on the elliptic function used to define them. Thus, skyrmion fields expressed in terms of the σ fields, *e.g.*, equation (5), evolve differently from those expressed through $\wp$, *e.g.*, equation (3). In the former case, energy chunks started off from rest stay still in their initial positions as time goes by. In the latter case, we have encountered novel phenomena like lump-splitting, scattering at ninety degrees and motion reversal, despite no initial speed being given to the systems. One of the aims of this research has been to investigate various properties of solitons on T_2 by employing alternative elliptic functions. Comparison of the various solitons generated by alternative elliptic functions (and with the lumps on $\Re_2$) may help us to gain a deeper insight into the CP^1 dynamics.

One of our main results is the existence of a mode of splitting a skyrmion into two lumps (though we have to work with two skyrmions which then split into four lumps). There clearly is a potential barrier which, when overcome, allows the skyrmions to divide up. We have managed to overcome this barrier by starting our simulations with a Skyrme initial condition which runs up to a $t = t_0$, when the Skyrme term is switched off: The evolution continues with $\theta_1 = 0$. Such an approach adds a little energy to the system and then transforms it to the mode responsible for overcoming the barrier. This barrier is a numerical artifact, brought about by the discretisation procedure.

The longer the system runs with $\theta_1 \neq 0$ the more energy is transferred; hence there seems to be a minimal time of such a simulation $t = t_0$ below which the skyrmions do not break up. This we have seen in our simulations – our estimates of t_0 gave us $t_0 \sim 1.25$.

In the present paper we have also learned that splitting takes place only when the parameter b in $W = \wp + b$ satisfies $b \in \Re - \{0\}$. For some values of b we have found that the forces operating in $\wp$-lump systems with $v_0 = 0$ either lead to head-on collisions and a subsequent 90° scattering or lead to a motion reversal. This property is qualitatively different to any other CP^1 structures that we know of.

The table below summaries some of our results:

Im(b)/Re(b)	$= 0$	$\neq 0$
=0	4 lumps on diagonals; breather	2 lumps on central cross; splitting
$\neq 0$	2 lumps on diagonals; 90° scattering	2 lumps elsewhere motion reversal

In future work we hope to report on:

- configurations with $v_0 \neq 0$ on the central cross to further analise the splitting phenomenon;
- lumps initially situated slightly off the central cross $[b = (\alpha, \beta),\ 0 < \beta \ll 1]$;
- lumps slightly off the main diagonals $[b = (\alpha, \beta),\ 0 < \alpha \ll 1]$;
- obtain deeper insight into motion reversal.

A look a bit farther ahead will necessarily include configurations with higher Brouwer degree, as well as states defined through other functions, *e.g.*, the elliptic ones of Jacobi and the pseudo-elliptic theta functions.

Part of this work was carried out when RJ Cova was on a research visit at the Department Mathematical Sciences of the University of Durham, and later when WJZ visited the Physics Department of La Universidad del Zulia. We thank the Royal Society of London and Venezuela's Conicit for supporting these visits. We are also grateful to both Universities for their hospitalities. CONDES project 01797-00 is also thankfully acknowledged.

References

1. *Proceedings of the Second Winter School on Math. Phys. "Physics in (2+1) dimensions", February 1991, Sorak Mountain Resort, Korea*, edited by Y.M. Cho (World Scientific, 1992).
2. T.H.R. Skyrme, Nucl. Phys. **31**, 556 (1962).
3. E. Witten, Nucl. Phys. B **223**, 422 (1983).
4. B. Piette, W. Zakrzewski, Chaos, Solitons, Fractals **5**, 2495 (1995).
5. R.J. Cova, W.J. Zakrzewski, Nonlinearity **10**, 1305 (1997).
6. R.J. Cova, Helv. Phys. Acta. **71**, 675 (1998).
7. J.M. Speight, Comm. Math. Phys. **194**, 513 (1998).
8. E. Goursat, *Functions of a complex variable* (Dover Publications, 1916).
9. D.F. Lawden, *Elliptic functions and applications* (Springer Verlag, 1989).
10. J.M. Speight, private communication.
11. R.J. Cova, Eur. Phys. J. B **15**, 673 (2000).
12. C. Rosenzweig, A. Mohan Srivastava, Phys. Rev. D **43** 12, 4029 (1991).
13. M. Atiyah, N. Hitchin, *The geometry and dynamics of magnetic monopoles* (Princeton University Press, 1988).
14. T. Samols, Comm. Math. Phys. **145**, 149 (1992).